

Engineering Notes

ENGINEERING NOTES are short manuscripts describing new developments or important results of a preliminary nature. These Notes should not exceed 2500 words (where a figure or table counts as 200 words). Following informal review by the Editors, they may be published within a few months of the date of receipt. Style requirements are the same as for regular contributions (see inside back cover).

Locating Sudden Changes in Heat Flux Using Higher Temporal Derivatives of Temperature

J. I. Frankel,* M. Keyhani,† R. V. Arimilli,‡ and J. Wu§
University of Tennessee, Knoxville, Tennessee 37996-2210

DOI: 10.2514/1.32585

Nomenclature

b	=	plate thickness, m
C	=	heat capacity, kJ/(kg°C)
k	=	thermal conductivity, W/(m°C)
L	=	length of the plate, m
N_n	=	n th normalization integral, m
n	=	dummy index in summation
q_i''	=	surface heat flux ($i = 0, 1, 2$), W/m ²
$q_s''(x, t)$	=	dimensional surface heat flux, W/m ²
$q_x''(x, t)$	=	dimensional axial heat flux, W/m ²
$T(x, t)$	=	dimensional temperature, °C
T_i	=	initial temperature, °C
T_o	=	boundary temperature at $x = 0$, °C
t	=	dimensional time, s
t_{\max}	=	maximum time, s
w	=	half-width of surface heat flux, m
x	=	dimensional space variable, m
x_1	=	half-length of the plate, m
y	=	dimensional space variable, m
z	=	dimensional space variable, m
α	=	thermal diffusivity, m ² /s
Δx	=	$x_1/10$, m
Δy	=	$w/4$, m
λ_n	=	n th eigenvalue, m ⁻¹
$\theta(x, y, t)$	=	dimensional temperature, °C
ρ	=	density, kg/m ³
$\Psi_n(x)$	=	n th eigenfunction associated with n th eigenvalue

I. Introduction

THIS Note presents some new observations that support the need to develop rate-based sensors for detecting sudden changes in heat flux that can be brought about in many physical problems of

Received 2 June 2007; accepted for publication 25 February 2008. Copyright © 2008 by the American Institute of Aeronautics and Astronautics, Inc. All rights reserved. Copies of this paper may be made for personal or internal use, on condition that the copier pay the \$10.00 per-copy fee to the Copyright Clearance Center, Inc., 222 Rosewood Drive, Danvers, MA 01923; include the code 0022-4650/08 \$10.00 in correspondence with the CCC.

*Professor, Mechanical, Aerospace and Biomedical Engineering Department; vfrankel@earthlink.net. Associate Fellow AIAA (Corresponding Author).

†Professor, Mechanical, Aerospace and Biomedical Engineering Department.

‡Professor, Mechanical, Aerospace and Biomedical Engineering Department. Senior Member AIAA.

§Assistant Professor, Electrical and Computer Engineering Department.

interest. To illustrate this important but subtle finding, this Note presents two examples that are indicative of practical physical processes. The first example describes a simplified model for hypersonic flow over a flat plate in which a sudden change in heat flux occurs at the transition point. Locating the point of transition in hypersonic flows is highly important and is identifiable by a sudden change in both heat flux and skin friction. In the one-dimensional transient-heat-conduction model for the plate, the surface heat flux appears in the heat equation. The second example considers a finite width surface heat flux impinging a two-dimensional half-space geometry. In this case, a strong sink is present and the effect of the geometrical dimensionality can be considered in the proposed observations. Both studies permit analytic solutions by classical methods. In particular, focus is directed to the spatial region near the jump discontinuity and the local behavior of the time derivatives of temperature. As noted by Frankel et al. [1–8], various types of inverse problems can also benefit from the development of rate-based sensors.

II. One-Dimensional Heat Conduction: Detecting Transition in a Flat Plate

Locating the position at which laminar–turbulent transition takes place in hypersonic flows is critical to the development of large airbreathing hypersonic vehicles [9]. The occurrence of transition is indicated by dramatic changes in heat transfer and skin friction. Figure 1 shows [9] the heat transfer (heat flux) distribution along a cone under reentry conditions. At the assumed transition onset point ($x/L = 0.65$), a large jump in heat flux is observed. Many methods for experimentally detecting transition are limited to laboratory conditions. Flowfield methods include [10] 1) hot-wire anemometry, 2) total (pressure) head measurements near the surface, 3) stethoscoping based on acoustics, 4) sublimation of surface coating, and 5) schlieren photography. Surface measurements involving temperature and heat flux are also used. In-flight conditions preclude the use of the five flowfield-method measurements. Future flight craft may require intelligent data collection for processing to optimize wing configurations and other advanced concepts. In-flight optimization will involve a combination of data collection, analysis, feedback, and actuation.

Figure 2 qualitatively displays high-speed flow over a flat plate. Let us assume that the plate is sufficiently thin to be able to lump in the y direction. Additionally, suppose that the solid circles could potentially represent thermal sensors (temperature or heating/cooling rate). To illustrate the concept of heating/cooling rate as a potential indicator for detecting transition, let us form a simplified one-dimensional transient-heat-conduction model in the flat plate shown in Fig. 2. The simplified linear heat equation is given as

$$\frac{1}{\alpha} \frac{\partial T}{\partial t}(x, t) = \frac{\partial^2 T}{\partial x^2}(x, t) + \frac{q_s''(x, t)}{kb} \quad x \in (0, L), \quad t > 0 \quad (1a)$$

subject to the boundary conditions

$$T(0, t) = T_o \quad (1b)$$

$$\frac{\partial T}{\partial x}(L, t) = 0 \quad t > 0 \quad (1c)$$

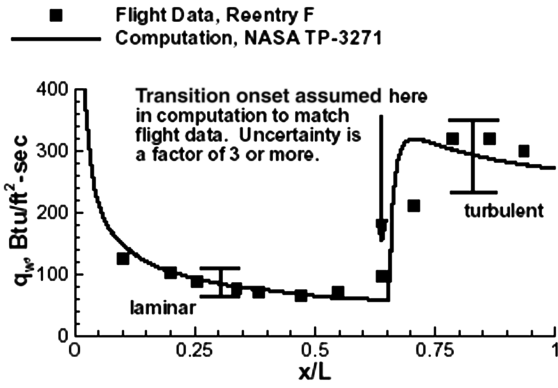


Fig. 1 Heat flux along a cone [9].

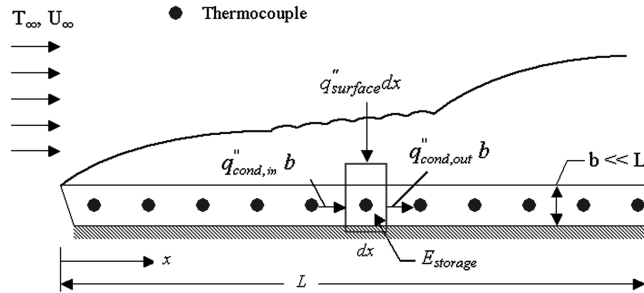


Fig. 2 Schematic of high-speed flow over a thin flat plate with indicated flow regimes.

and the initial condition

$$T(x, 0) = T_i \quad x \in [0, L] \quad (1d)$$

where T is the temperature; (x, t) are the independent variables for space and time, respectively; $q''_s(x, t)$ is the surface heat flux; b is the thickness of the plate; L is the length of the plate ($b \ll L$); k is the thermal conductivity; α is the thermal diffusivity of the plate; and T_i and T_o are, respectively, the initial uniform-temperature and imposed constant-temperature boundary conditions at $x = 0$. Further, assume $T_i < T_o$ and let the source function $q''_s(x, t)$ be described by the two-part formula

$$q''_s(x, t) = \begin{cases} q''_1, & 0 \leq x \leq x_1 \\ q''_2, & x_1 < x \leq L \end{cases} \quad (2)$$

Alternatively, Eq. (1a) can be viewed as a slab of width L having a volumetric heat source given by $q''_s(x, t)/b$. The proposed two-part formula for the surface heat flux shown in Eq. (2) is merely an idealized model of the sudden jump condition described in Fig. 1. For analytic simplicity, this steady-state source is imposed to obtain an analytic solution. For early times, the effect of the boundaries in a long plate near the center point $x = x_1 = L/2$ is small, and hence this choice is merely made for convenience. The solution to this linear nonhomogenous heat equation is obtained by using the finite integral transform technique [11]. Using this approach, we obtain the exact solution

$$T(x, t) = T_o + (T_i - T_o) \sum_{n=0}^{\infty} \frac{\Psi_n(x) e^{-\alpha \lambda_n^2 t}}{\lambda_n N_n} + \frac{1}{kb} \sum_{n=0}^{\infty} \frac{\Psi_n(x)}{\lambda_n^3 N_n} (1 - e^{-\alpha \lambda_n^2 t}) \left[(q''_2 - q''_1) \cos(\lambda_n x_1) + q''_1 \right] \quad (3)$$

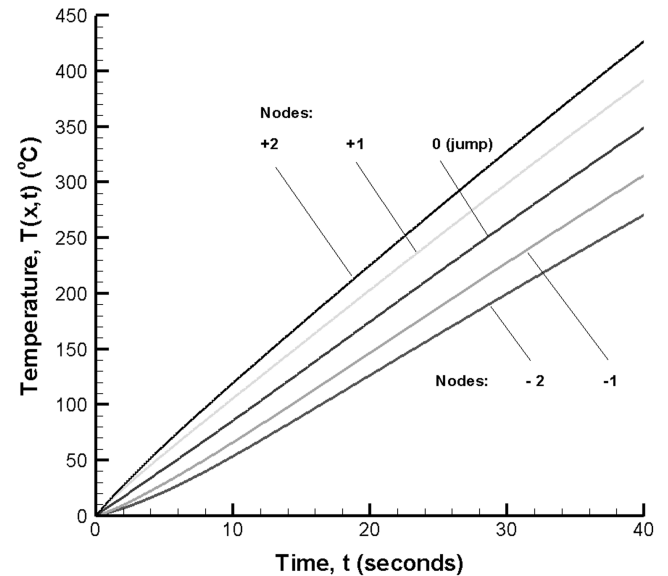
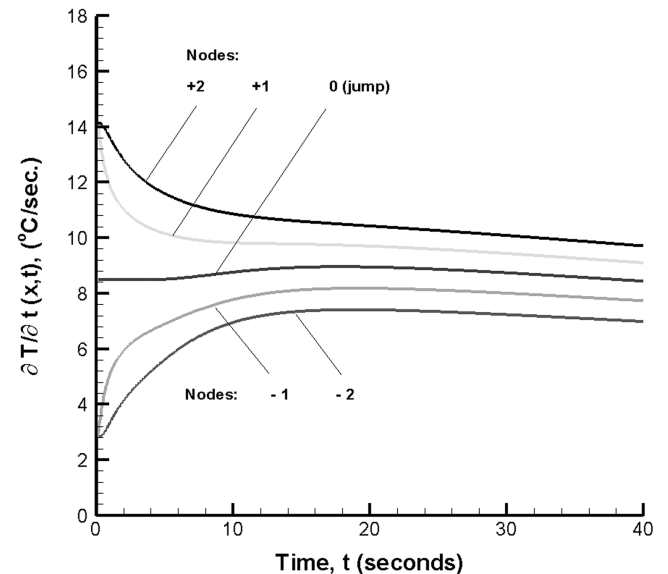
$$x \in [0, L], \quad t \geq 0$$

where the eigenvalues are $\lambda_n = (2n + 1)\pi/(2L)$, the eigenfunctions are $\Psi_n(x) = \sin(\lambda_n x)$, and normalization integrals reduce to $N_n = L/2$ ($n = 0, 1, \dots$). For the moment, let us assign geometrical and

physical properties to this example based on pure copper. Let the thermophysical properties of the plate be assigned as $k = 386 \text{ W/(m}^\circ\text{C)}$, $\rho = 8890 \text{ kg/m}^3$, and $C = 398 \text{ J/(kg}^\circ\text{C)}$, in which the thermal diffusivity can be calculated as $\alpha = k/(\rho C)$. Next, let the geometrical properties be given as $L = 0.25 \text{ m}$, $b = 0.01 \text{ m}$, and $x_1 = L/2$. Finally, let $q''_1 = 0.1 \text{ MW/m}^2$, $q''_2 = 5 \times q''_1$, $T_i = 0^\circ\text{C}$, $T_o = 100^\circ\text{C}$, and $t_{\max} = 40 \text{ s}$.

Figures 3–5 display the time histories of temperature $T(x, t)$, the heating/cooling rate $(\partial T/\partial t)(x, t)$, and the second time derivative of temperature $(\partial^2 T/\partial t^2)(x, t)$ about the point $x = x_1 = L/2$ (location at which the surface heat-flux discontinuity is imposed), to indicate the sensitivity of each function in proximity to the sudden change of surface energy deposition. The second time derivative of temperature is presented for several reasons, including the following:

- 1) This term can physically appear in the study of thermoelasticity ([12], p. 57) involving Fourier heat conduction in elastic solids.
- 2) This term can potentially be measured with the aid of bimaterial microcantilever beams.

Fig. 3 Temperature histories about the heat-flux discontinuity location $x = x_1$: negative (left) or positive (right).Fig. 4 First-time derivative of temperature about the heat-flux discontinuity location $x = x_1$: negative (left) or positive (right).

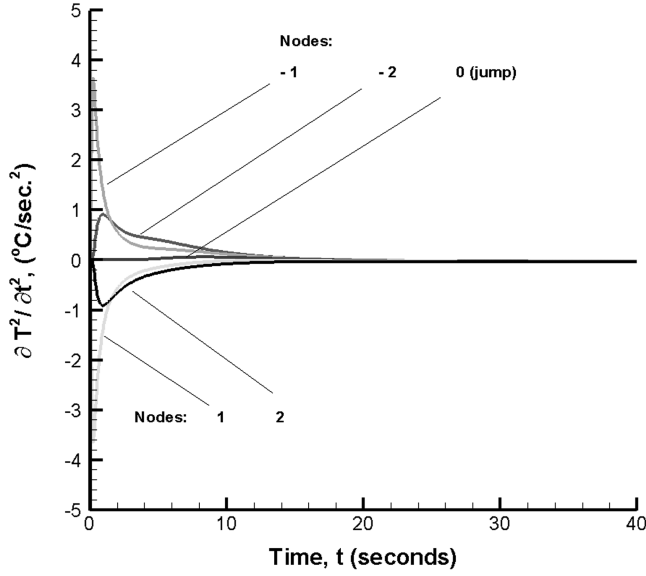


Fig. 5 Second-time derivative of temperature about the heat-flux discontinuity location $x = x_1$: negative (left) or positive (right).

3) This term will be shown to have physical significance (see Fig. 5).

Figures 3 and 4 display the time histories of temperature $T(x, t)$ and the heating rate $(\partial T/\partial t)(x, t)$ about the point $x = x_1 = L/2$ (location at which the surface heat-flux discontinuity is imposed), respectively, to indicate the sensitivity of each function due to the surface heat flux. The temperature-history lines nearly run parallel when early time histories about point x_1 have different concavities. Here, the node number is given as position left (negative) or right (positive): that is, $\text{node}_j = x_1 + j\Delta x$, where the distance between two consecutive nodes is given as $\Delta x = x_1/10 = 1.25$ cm. Figure 4 displays the corresponding heating/cooling rate at the indicated sensor sites about the imposed surface jump in energy deposition. Hence, the heating/cooling rate presents an amplified early time view, whereas the temperature itself appears to be of questionable value. Additionally, if sufficient noise were to take place in the temperature sensors at low temperature, it would be difficult to discern signals at the various sensor sites. The concavity change displayed in Fig. 5 about the transition point also suggests that the second derivative, $(\partial^2 T/\partial t^2)(x, t)$, should produce a sign change about the transition location, as shown in Fig. 5. These observations are quite suggestive and should lead to an aggressive pursuit to develop temperature-rate sensors for use in locating transition in hypersonic flows. Therefore, a real-time check on the sign of the signals from a set of $(\partial^2 T/\partial t^2)(x, t)$ would readily reveal that the transition point is located between the two consecutive in-situ thermocouples.

III. Two-Dimensional Heat Conduction: Detecting Flux Discontinuity

Increasing the physical dimensionality of the problem permits geometrical and diffusive effects to be considered on the surface temperature and its time derivatives. Next, consider the physical situation described in Fig. 6 and mathematically prescribed by the two-dimensional constant-property heat equation:

$$\frac{1}{\alpha} \frac{\partial \theta}{\partial t}(x, y, t) = \frac{\partial^2 \theta}{\partial x^2}(x, y, t) + \frac{\partial^2 \theta}{\partial y^2}(x, y, t) \quad (4a)$$

$$x \in (0, \infty), \quad y \in (-\infty, \infty), \quad t > 0$$

where $\theta(x, y, t)$ is dimensional temperature subject to the boundary conditions

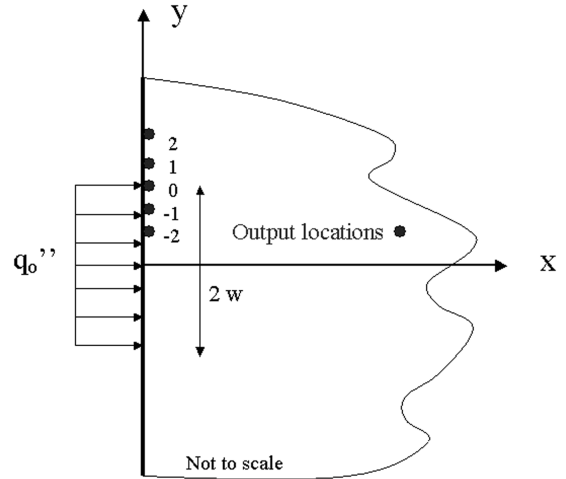


Fig. 6 Half-space schematic displaying surface heat flux.

$$-k \frac{\partial \theta}{\partial x} = \begin{cases} q''_0, & |y| \leq w \\ 0, & |y| > w \end{cases} \quad (4b)$$

$$\lim_{x \rightarrow \infty} \theta(x, y, t) = T_i \quad (4c)$$

$$\lim_{y \rightarrow \pm \infty} \theta(x, y, t) = T_i, \quad t > 0 \quad (4d)$$

and the initial condition

$$\theta(x, y, 0) = T_i, \quad x \in (0, \infty), \quad y \in (-\infty, \infty) \quad (4e)$$

The surface heat flux has a width of $2w$ and magnitude of q''_0 . For simplicity, let $T_i = 0^\circ\text{C}$, then the resulting surface temperature distribution is analytically provided as [13]

$$\theta(0, y, t) = \frac{q''_0 \sqrt{\alpha}}{\sqrt{\pi k}} \left(\sqrt{t} \left(\text{erf} \left(\frac{y+b}{2\sqrt{\alpha t}} \right) + \text{erf} \left(\frac{b-y}{2\sqrt{\alpha t}} \right) \right) + \frac{y+b}{2\sqrt{\alpha \pi}} \Gamma \left(0, \frac{(y+b)^2}{4\alpha t} \right) + \frac{b-y}{2\sqrt{\alpha \pi}} \Gamma \left(0, \frac{(b-y)^2}{4\alpha t} \right) \right), \quad (5)$$

$$y \in (-\infty, \infty), \quad t \geq 0$$

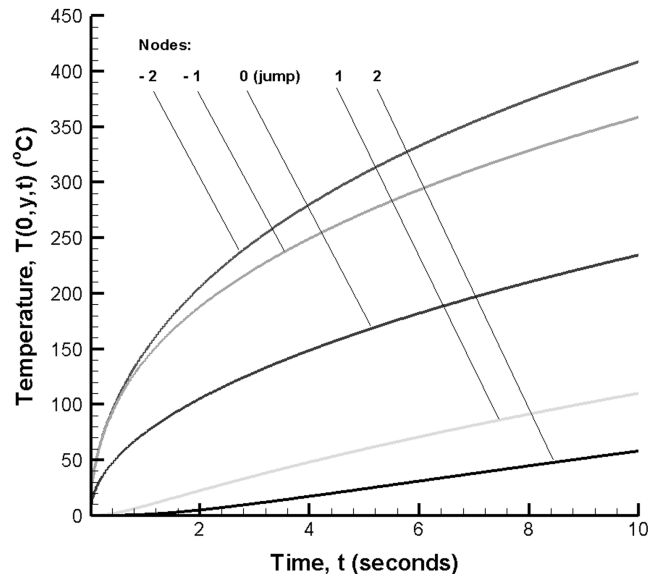


Fig. 7 Temperature histories about the heat-flux discontinuity location $y = w$ for stainless steel.

where $\text{erf}(z)$ is the error function [14] and $\Gamma(0, z)$ represents the incomplete gamma function [14]. Analytic time differentiation of Eq. (5) can be performed to obtain higher time derivatives of temperature at the surface. For definiteness and contrast, two diverse materials are considered in this analysis. Let $w = 1$ cm, and the nodes about the discontinuous heat flux are given by $y_j = w + j\Delta y$, where $\Delta y = w/4 = 0.25$ cm and $j = -2, -1, 0, 1, 2$.

Figures 7–9 present results based on assuming stainless steel properties of $k = 14.7$ W/(m°C), $\alpha = 3.75 \times 10^{-6}$ m²/s, $q''_0 = 10^6$ W/m², and $t_{\max} = 10$ s, and Figs. 10–12 present results based on assuming copper properties of $k = 386$ W/(m°C), $\alpha = 1.091 \times 10^{-4}$ m²/s, $q''_0 = 10^7$ W/m², and $t_{\max} = 1$ s. This geometry presents an extremal case, because an infinite sink is present. The previous study represented an extremal case in which energy could only be propagated in a single dimension.

Figure 7 displays the stainless steel temperature histories $T(0, y, t)$ about point $y = w$, when the surface heat flux jumps from a high level of energy impingement to zero. Both x – y diffusive effects appear in Figs. 7–9 due to this geometry. This geometry offers a

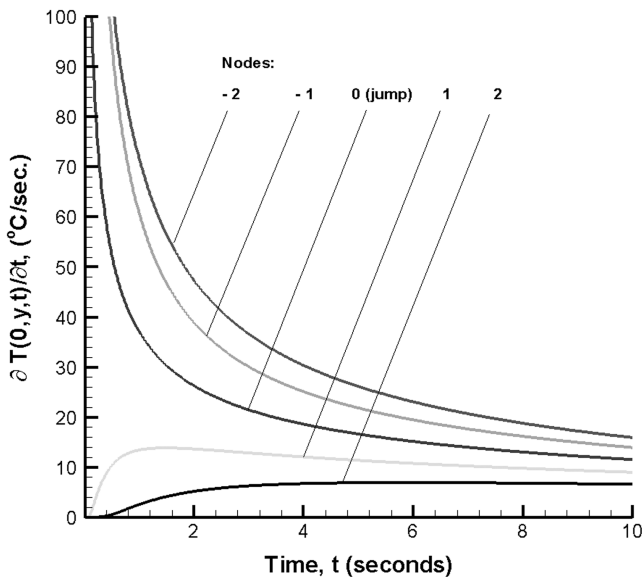


Fig. 8 First-time derivative of temperature about the heat-flux discontinuity location $y = w$ for stainless steel.

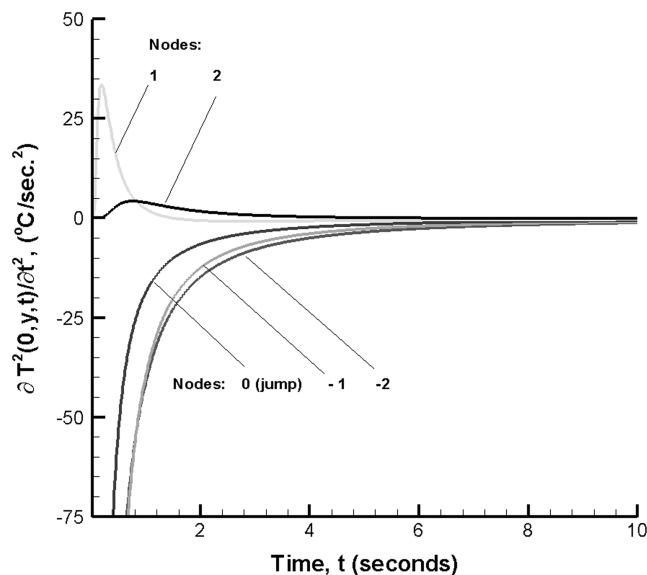


Fig. 9 Second-time derivative of temperature about the heat-flux discontinuity location $y = w$ for stainless steel.

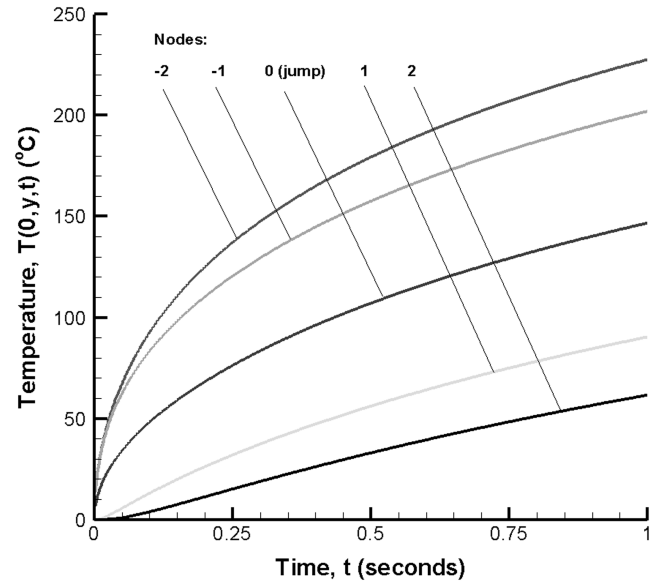


Fig. 10 Temperature histories about the heat-flux discontinuity location $y = w$ for copper.

significant sink in both the x and y directions. The effect of geometry allows for some graphical separation of temperature between nodes. Figure 8 shows the heating-rate histories $(\partial T/\partial t)(0, y, t)$ over time. This figure strongly implies that the point at which the jump condition occurs lies between nodes ± 1 without requiring much insight or interpretation. Figure 9 presents $(\partial^2 T/\partial t^2)(0, y, t)$ histories of the nodes about the discontinuity. For early times, a definite sign change occurs, indicating a sudden change in flux.

Figures 10–12 illustrate a set of figures that is similar to the set shown in Figs. 7–9, but now with consideration to copper, for which the time scale is decreased and the surface heat flux is increased. Figure 9 displays the temperature histories about the $y = w$ location. Figure 10 presents the heating rate $(\partial T/\partial t)(0, y, t)$ over time and again provides a discriminating feature. Figure 12 presents $(\partial^2 T/\partial t^2)(0, y, t)$ histories of the nodes about the discontinuity. For early times, a definite sign change occurs, indicating a sudden change in flux, narrowing down the field of potential locations. It appears quite possible to estimate the location of the *sharp and sudden* jump between two or three thermocouples.

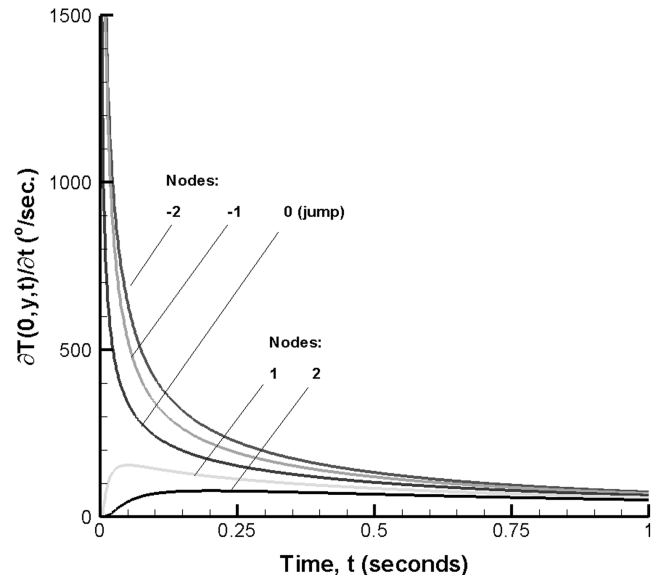


Fig. 11 First-time derivative of temperature about the heat-flux discontinuity location $y = w$ for copper.

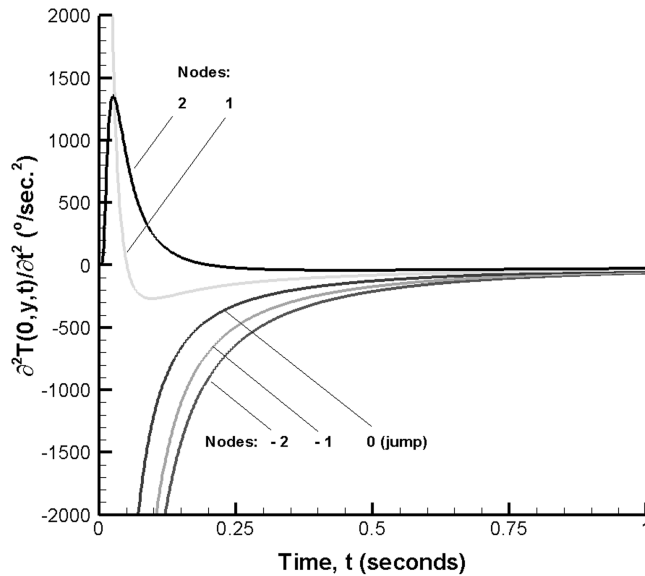


Fig. 12 Second-time derivative of temperature about the heat-flux discontinuity location $y = w$ for copper.

IV. Conclusions

The purpose of this Note involves relating an observation useful for detecting sudden changes in heat flux through either 1) the careful analysis of higher time derivatives of temperature or 2) the direct and instantaneous measurement of the time derivative of temperature. As with mechanical systems, it is often better to measure acceleration than displacement. This analogy also holds true for thermal systems. It is well known that numerical differentiation of raw data is ill-posed [15–17], and this is especially noticeable as the sample size is increased for a fixed time span. Measurement of acceleration can be performed without differentiation and thus one postulates that sensors capable of measuring higher time derivatives [8] of temperature are thus conceivable and could impact aerospace heat transfer studies.

Acknowledgment

The work described here was developed with National Science Foundation support (CBET-0601236).

References

[1] Frankel, J. I., and Keyhani, M., "Inverse Heat Conduction: The Need of $\partial T / \partial t$ Data for Design and Diagnostic Purposes," Model and Identification Conference (MIC 99), International Association of Science and Technology for Development Paper 124, Calgary, Alberta, Canada, Feb. 1999.

- [2] Frankel, J. I., "Inverse Heat Conduction and Data-Type Issues," *Boundary Element Communications*, Vol. 11, No. 4, 2000, pp. 37–42.
- [3] Frankel, J. I., Osborne, G. E., and Taira, K., "Stabilization of Ill-Posed Problems Through Thermal Rate Sensors," *Journal of Thermophysics and Heat Transfer*, Vol. 20, No. 2, 2006, pp. 238–246. doi:10.2514/1.9136
- [4] Frankel, J. I., and Lawless, J. J., "Numerically Stabilizing Ill-Posed Moving Surface Problems Through Heat Rate Sensors," *Journal of Thermophysics and Heat Transfer*, Vol. 19, No. 4, 2005, pp. 587–592. doi:10.2514/1.11057
- [5] Frankel, J. I., "Regularization of Inverse Heat Conduction by Combination of Rate Sensors Analysis and Analytic Continuation," *Journal of Engineering Mathematics*, Vol. 57, No. 2, 2007, pp. 181–198. doi:10.1007/s10665-006-9073-y
- [6] Frankel, J. I., and Osborne, G. E., "Motivation for the Development of Heating/Cooling Rate dT/dt and Heat Flux Rate dq/dt Sensors for Engineering Applications," 42nd AIAA Aerospace Sciences Meeting and Exhibit, Reno, NV, AIAA Paper 2004-823, Jan. 2004.
- [7] Frankel, J. I., "Heating/Cooling Rate Sensor Development for Stable, Real-Time Heat Flux Predictions," 43rd AIAA Aerospace Sciences Meeting and Exhibit, Reno, NV, AIAA Paper 2005-764, Jan. 2005.
- [8] Frankel, J. I., Arimilli, R. V., Keyhani, M., and Wu, J., "Heating Rate dT/dt Measurements Developed from In-Situ Thermocouples Using a Voltage-Rate Interface for Advanced Thermal Diagnostics," 25th AIAA Aerodynamics Measurement Technology and Ground Testing Conference, AIAA Paper 2006-3636, San Francisco, June 2006.
- [9] Schneider, S. P., "Hypersonic Laminar-Turbulent Transition on Circular Cones and Scramjet Forebodies," *Progress in Aerospace Sciences*, Vol. 40, Nos. 1–2, 2004, pp. 1–50. doi:10.1016/j.paerosci.2003.11.001
- [10] Kuethe, A. M., and Chow, C.-Y., *Foundations of Aerodynamics*, 4th ed., Wiley, NY, 1986, pp. 378–380.
- [11] Ozisik, M. N., *Heat Conduction*, Wiley, New York, 1980, pp. 522–593.
- [12] Boley, B. A., and Weiner, J. H., *Theory of Thermal Stresses*, Dover, New York, 1997, pp. 55–57.
- [13] Frankel, J. I., Keyhani, M., Arimilli, R. V., and J. Wu, "A New Multidimensional Integral Relationship Between Heat Flux and Temperature for Direct Internal Assessment of Heat Flux," *Zeitschrift für Angewandte Mathematik und Physik* (to be published). doi:10.1007/s00033-007-6135-6
- [14] Abramowitz, M., and Stegun, I. A., (eds.), *Handbook of Mathematical Functions*, Dover, New York, 1972, p. 260, 297.
- [15] Hanke, M., and Scherzer, O., "Inverse Problems Light: Numerical Differentiation," *American Mathematical Monthly*, Vol. 108, No. 6, 2001, pp. 512–520. doi:10.2307/2695705
- [16] Groetsch, T., "Differentiation of Approximately Specified Functions," *American Mathematical Monthly*, Vol. 98, No. 9, 1991, pp. 847–850. doi:10.2307/2324275
- [17] Frankel, J. I., Keyhani, M., and Taira, K., "In-Phase Error Estimation of Experimental Data and Optimal First Derivatives," *AIAA Journal*, Vol. 42, No. 5, 2004, pp. 1017–1024. doi:10.2514/1.9593

G. Palmer
Associate Editor